Heat Mass Transfer (2018) 54:773–784
DOI 10.1007/s00231-017-2146-9

ORIGINAL

Numerical study of silica-water based nanofluid nucleate pool boiling by two-phase Eulerian scheme

H. Salehi[1] · **F. Hormozi**[1]

Received: 12 March 2017 / Accepted: 22 August 2017 / Published online: 1 October 2017

Abstract In this research, numerical simulation of nucleate pool boiling of water and water–silica nanofluid was investigated using Eulerian multiphase approach. At first, nucleate pool boiling of pure water was simulated. Classic heat flux partitioning (HFP) model was used for the prediction of bubble parameters. To validate proposed approach, numerical results were compared with experimental data. In the next step, this scheme has been used for water-silica nanofluid. Due to dilute nanofluid (0.1% volume) concentration, it was assumed as a homogenous liquid and therefore, a two-phase approach was applied to simulate its boiling. Meanwhile, various correlations were compared to determine nucleation site density and bubble departure frequency and the best equation was found. Results demonstrated nanoparticle deposition on the heater surface was a key factor that could change the heat transfer performance in boiling nanofluid. Therefore, accurate investigation of bubble behavior in nucleate boiling of nanofluids is a necessary concern to be focused in future modeling studies.

Nomenclature

g	gravitational acceleration (m/s2)
E	total energy of phase (j)
k	conductivity (w/m K)
T	temperature (K)
P	pressure (Pa)
t	time (s)
F	body force
h_{fg}	latent heat (kJ/kg)
C_D	Drag coefficient
Re	Reynolds number
Pr	prantle number
C_p	heat capacity (j/kg.k)
Γ_{kj}	interfacial mass transfer (kg m − 3 s−
q	heat flux (w/m2)
d_b	bubble departure diameter (mm)
f	bubble departure frequency (1/s)
Na	active nucleation site density (m^{-2})
t_w	bubble waiting time (ms)

Greek

ρ	density (kg/m3)
μ	dynamic viscosity (kg/m s)
α	volume fraction
σ	surface tension (N/m)

Subscripts

sat	saturated
v	vapor
l	liquid
s	solid
nf	nanofluid
np	nanoparticles
bf	base fluid

1 Introduction

The concept of nanofluids was firstly suggested by Choi [1]. They are defined as a type of fluids in which nano-scale particles are dispersed in conventionally basic fluids such as water, oil, and acetone. Nowadays, nanofluids are widely used in heat

✉ F. Hormozi
fhormozi@semnan.ac.ir

[1] Faculty of Chemical, Petroleum and Gas Engineering, Semnan University, Semnan, Iran

transfer media in many industrial fields such as nuclear power plants [2], thermosyphon [3], and air conditioning systems [4] because dispersed nanoparticles can significantly enhance the thermal performance of fluids.

Nucleate pool boiling of nanofluid involves a high rate of heat transfer. In recent decay, there is disagreement about the heat transfer rate in pool boiling although employing boiling of heat transfer still faces many challenges.

Das et al. [5] and You et al. [6] introduced the investigations of boiling nanofluids. Afterwards, many researchers conducted experimental or numerical studies to reveal the mechanisms of dramatic heat transfer performances and novel phenomena observed in boiling nanofluids. To enhance colloidal stability and to neglect variations in physical properties of boiling nanofluid, dilute concentrations (less than 0.1 v%) have higher priority. Kim et al. [7] measured the thermo-physical property of dilute aqueous nanofluid and found that the saturation temperature of nanofluids was varied within ±1 °C of that of pure water while the surface tension, thermal conductivity and viscosity differ negligibly. Therefore a dilute nanofluid behaves hydrodynamically like its base fluid and can be numerically treated as a single liquid phase despite the existence of two phases. These nanofluids increased the critical heat flux (CHF) up to 200%.

Milanona and Kumar [8] conducted experimental investigation of pool boiling with several nanofluids such as silica, alumina and ceria (CeO_2). The effect of PH alteration in their experiments was studied. Most of the experiments showed that boiling heat transfer has deteriorated. Troung [9] fulfilled experimental study with Al_2O_3 and SiO_2 water-based nanofluids. Results revealed approximately 70% improvement in the heat transfer rate. The pool boiling heat transfer of aqueous multi-walled carbon nanotube nanofluids on modified surfaces was experimentally investigated up to the critical heat flux by Sarafraz and Hormozi [10]. Results demonstrated that the pool boiling heat transfer coefficient on the plain surface decreased while it was enhanced for micro-finned surfaces. Dogan Ciloglu et al. [11] surveyed a comprehensive review of recent researches on nanofluids pool boiling. First, they briefly explained the development of nanofluids and their potential applications. They then discussed the effects of various parameters on nanofluids pool boiling. They concluded that the pool boiling heat transfer behavior of nanofluids depends on several parameters including the thermo-physical properties of nanofluids and the boiling surface properties, as well as their mutual interactions.

Despite using dilute nanofluid in nucleate pool boiling, it has been revealed the physical properties of nanofluid did not enhance the heat transfer. Rather, surface modification during the microlayer evaporation is the main reason of the enhancement in heat transfer [12]. When the microlayer vaporizes, nanoparticles dispersed in nanofluids deposit on the surface, improving the surface wettability and affecting the heat transfer performance. This mechanism is depicted in Fig. 1.

Development of a predictive powerful model for the system design and performance assessment by boiling is of great demand. Therefore, fundamental investigations are urgently needed to develop a predictive model for nucleate boiling of nanofluids. Because of near-molecular mixing between nanofluid and the pure basic liquid, a nanofluid hydro-dynamically behaves like its pure basic fluid and therefore, single phase modeling of nanofluid is reasonable [13]. Several investigations have revealed that the single-phase computational fluid dynamics (CFD) model can describe the flow and heat transfer behavior of nanofluid without any phase change on the conditions that the physical properties are formulated [14].

Nucleate boiling of pure water alone is an extremely complicated physical phenomenon. Also, nanoparticles in the base liquid strengthen the complexity. Meanwhile some studies that have investigated several recent phenomena such as surface modification [7], flow correction [15] and concludedthat the surface correction seems to be the main reason of the considerable boiling heat transfer enhancement of nanofluids.

For the first time, nucleate pool boiling heat transfer of nanofluid was numerically evaluated by Aminfar et al. [16]. They employed two-phase and three-phase mixture models for silica and alumina water based nanofluids. They reported that simulated results were in good agreement with experimental data. Also, they concluded that two-phase simulations containing effective parameters were more accurate than three-phase simulations. Ganapathy and Sajith [17] suggested a composite, semi-analytical model to investigate various effects of particle deposition on heater surface such as correction in surface wettability, surface roughness and increased resistance in the pool boiling. Results showed that the effects of change in surface wettability were explained by the change in surface roughness.

For nucleate boiling, bubble nucleation at heating section is the source of void in the bulk liquid. Therefore, it is essential to model heat and mass transfer on the heater surface as a boundary condition for the purpose of an exact two-fluid modeling. During the past few years, heat flux partitioning (HFP) model proposed by Renssler Polytechnic Institute (RPI) model [18] has been extensively employed to describe heat and mass transfer on the heater surface with nucleate boiling. Two-fluid modeling of nucleate boiling of dilute

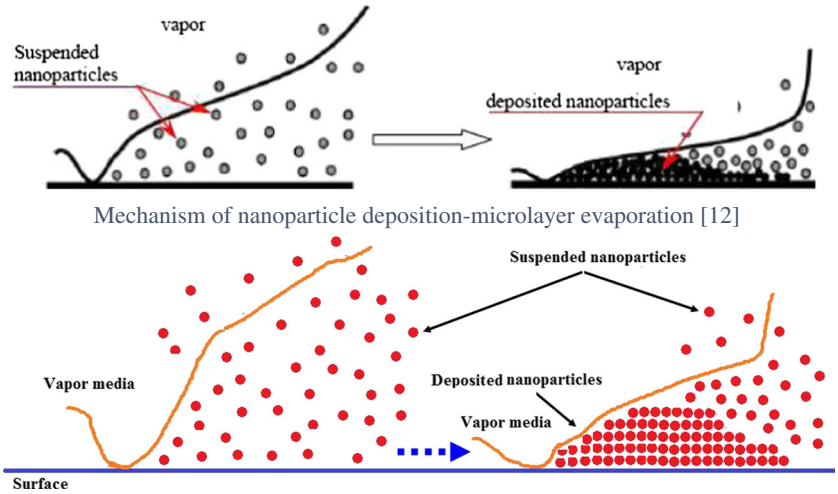

Fig. 1 a Mechanism of nanoparticle deposition-microlayer evaporation [12]. b Mechanism of nanoparticles concentrating in microlayer evaporation

water-silica nanofluid was numerically studied by Xiangdong Li et al. [19]. They investigated the effects of changed liquid property, active site density and bubble departure diameter boiling heat transfer. Due to the complexicity of surface morphology correction including that by nanoparticles, this subject requires more thorough study. Also, Xiandong Li et al. [20] assessed nucleate boiling of nanofluid by heat flux partitioning (HFP) model. They employed new closure correlation for nucleation site density, bubble departure diameter and frequency. 2-D computation domain was selected to analyze the effects of surface wettability and nanosize of material. The results ascertained that HFP model attained satisfactory agreement with data existing in the literature. Valizadeh and Shams [21] numerically fulfilled the water-based nanofluid subcooled flow boiling by three-phase modeling. They employed bubble parameters related to pure water in their model. The numerical results from the nanofluid boiling modeling were compared with experimental data in the literature and good agreement was observed.

To best of our knowledge, there is still not a precise predictive correlation for behavior of nucleate boiling for nanofluids. Available correlations have been presented for certain conditions and the deviation has not been negligible in some cases. Therefore, further studies is needed in this field. In the present study, an attempt is made to consider the effective correlations for HFP model. In each step, the results of simulation are compared with experimental data reported by Gerardi et al. [22], selecting the best model.

2 Theoretical formulation for nucleate boiling of nanofluid

In the Eulerion multiphase scheme (two-fluid model) boiling, the liquid behaves as the continuous phase and vapor bubbles are the disperse phase. As previously mentioned, due to near-molecular mixing between dilute nanofluid and the pure base liquid, a nanofluid hydro-dynamically behaves like its pure base fluid and therefore, single phase modeling of nanofluid is reasonable.

Two sets of conservation equations governing the balance of mass, momentum and energy of each phase are considered which are presented as follows:

2.1 Eulerian two-fluid model

Continuity, momentum and energy equations for two-fluid model are as follows [21]:

Continuity equation:

$$\frac{\partial(\rho_k\alpha_k)}{\partial t}+\nabla.(\rho_k\alpha_k v_k)=\Gamma_{kj} \tag{1}$$

Momentum equation:

$$\frac{\partial(\rho_k\alpha_k v_k)}{\partial t}+\nabla.(\rho_k\alpha_k v_k v_k)=\alpha_k\nabla P+\rho_k\alpha_k g+\nabla\left[\alpha_k\mu_k^e\left(\nabla v_k+(\nabla v_k)^T\right)\right]+\left(\Gamma_{kj}v_k+\Gamma_{jk}v_j\right)+F_{kj} \tag{2}$$

Energy equation:

$$\frac{\partial(\rho_k\alpha_k E_k)}{\partial t}+\nabla.(\rho_k\alpha_k v_k E_k)=\nabla\left[\alpha_k k_k^e(\nabla T_k)\right]+\left(\Gamma_{kj}E_k+\Gamma_{jk}E_j\right)+F_{kj} \tag{3}$$

Where the subscripts of k and j are phase denotations (k,j = l for liquid phase and k, j = v for vapor phase).

In these equations $\Gamma_{kj}$is the interfacial mass transfer in the liquid phase on the surface heater. In the bulk liquid this quantity is equal to zero. This is because pool boiling begins at saturation temperature.

$(\Gamma_{kj}v_k + \Gamma_{jk}v_j)$ in the momentum equation represents the momentum transfer due to liquid evaporation or vapor condensation.

Also, $(\Gamma_{kj}E_k + \Gamma_{jk}E_j)$ in the energy equation stands for the energy transfer due to phase change.

2.2 Modeling of interfacial transfer mechanism

For solving the governing equations, the interfacial transfer consists of interfacial momentum, heat and mass transfer are required.

For the viscous model, the two flow regimes are laminar and turbulent albeit with different models. Due to the chaotic nature of vapor bubbles and the boundary layer disruption due to bubble formation and departure, multiphase flow is intrinsically turbulent in nature. Therefore, all numerical simulations were performed using one of the turbulent solvers, in particular a form of the two-equation k-ε model, where k is the turbulent kinetic energy and ε is the turbulent dissipation rate. Various models of k-ε were investigated: standard, realizable and renormalization group (RNG) [23].By applying standard k-ε model, considerable deviation was not observed so it was selected., The standard k-ε model is the least expensive model in terms of computational cost while the realizable k-ε model is the most computationally expensive. Accordingly, the Sato eddy viscosity [24] was selected to model the turbulence because of vapor bubbles on the liquid phase.

In the vapor-liquid flows, each phase interacts with other phases. Two forces are included in the interaction of two phases: drag and turbulent dispersion. The Schiller-Naumann correlation was selected for drag force. A turbulent dispersion force has been considered to take into account the turbulence assisted bubble dispersion. To model the turbulent dispersion force, Favre averaged drag force (FAD) was used [25].

$$F_{disp} = -\frac{3C_D\mu_l}{4d_B\sigma_l}(v_v - v_l)\frac{\nabla\alpha_v}{1-\alpha_v} \tag{4}$$

Heat transfer between vapor and liquid phases occurs due to thermal non-equilibrium across the phase interface. A common model for interface heat transfer considers separate heat transfer processes either side of the phase interface. This model was named the two-resistance heat transfer model. In the present study, Ranz-Marshall model was employed to calculate the liquid phase heat transfer [26] in which a zero-resistance condition was applied for the vapor phase. The Ranz-Marshall correlation is presented by the following expression:

$$Nu_p = 2 + 0.6Pr_q^{1/3}Re_p^{1/2} \tag{5}$$

2.3 Interface mass transfer by heat flux partitioning (HFP) as modal

The HFP model proposed by Kural and Podowski [27] was employed for mass transfer mechanism between two phases. In fact, the HFP model was incorporated as a boundary condition in wall boiling model. According to this model, the heat flux from a heater surface is transferred into the liquid through three mechanisms, namely the evaporation, single phase turbulent convection and quenching (transient conduction) as following:

$$q = q_c + q_q + q_e \tag{6}$$

Where, q_e, q_q and q_c represent the heat flux components transferred by evaporation, quenching, and natural convection, respectively.

$$q_e = \frac{\pi}{6}d_{bw}^3\rho_v f N_a h_{fg} \tag{7}$$

$$q_q = \frac{2}{\sqrt{\pi}}fA_q\sqrt{t_w\lambda_l\rho_l c_{p,l}}(T_w - T_l) \tag{8}$$

$$q_c = A_c St\rho_l c_{p,l}v_l(T_w - T_l) \tag{9}$$

Mechanism of wall boiling with HFP model was schematically shown in Fig. 2.

where, d_{bw}, f, N_a, t_w, A_c and A_q are the bubble departure diameter, bubble departure frequency, active nucleation site density, bubble waiting time, the area fractions of the heater surface subjected to convection and quenching, respectively. A number of correlations are available in the literature and some of which have been fully validated for boiling of pure liquids, however, their applicability to nanofluids is still open to question. For the purpose of effective modeling, the nucleate boiling parameters should be carefully formulated. Therefore, the main goal of this research is the investigation of several correlations for d_{bw}, f and N_a. The results are then compared with the experimental data reported by Gerardi [22] to select the best correlation.

In nucleate boiling flow, bubbles are formed at the pit of surface heater which is known as the nucleation site. N_a is the active nucleation site density in the nucleate boiling, f is the frequency of bubbles that

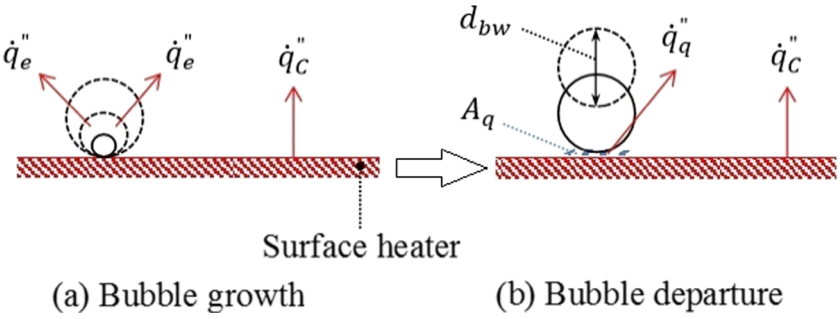

Fig. 2 Schematic of bubble growth and bubble departure in pool boiling according to HFP model

generates at the surface. When the bubbles reach a certain size, they are released from the surface and other bubbles start to take shape. This size is defined as the bubble departure diameter.

The active nucleation site density has been widely correlated to the wall superheat and some other parameters such as the liquid contact angle and the surface roughness.

Eq. (10) is used for the active nucleation site density depending on wall superheat, i.e. the temperature rise of the wall compared to the saturation temperature of the pool. This correlation was proposed by Kocamustafaogullari and Ishii [26].

$$N_a = \frac{f(\rho^*) r_c^{*4.4}}{d_b} \tag{10}$$

Where

$$r_c^* = 2\frac{r_c}{d_{bw}}, \tag{11}$$

$$r_c = \frac{2\sigma T_{sat}}{\rho_v h_{fv} \Delta T_{sap}}, \tag{12}$$

$$\rho^* = \frac{\rho_l - \rho_v}{\rho_v} \tag{13}$$

$$f(\rho^*) = 2.157 \times 10^{-7} \rho^{*-3.2} \left(1 + 0.0049\rho^*\right)^{4.13} \tag{14}$$

Ganapathy and Sajith [17] suggested a semi analytic model for active site density. In this correlation, the effect of nanoparticle deposition on bubble nucleation was described. In Eq. (15) the wettability enhancement and the nanoparticle size relative to the surface roughness were regarded.

$$N_a = 218.8 \frac{1}{\gamma} Pr_l^{1.63} \left(\left(14.5 - 4.5 \left(\frac{PR_a}{\sigma} \right) + 0.4 \left(\frac{PR_a}{\sigma} \right)^2 \right) \beta^{-3} \left(\frac{R_a}{d_p} \right)^{-0.5} \right)^{-0.4} \Delta T_{sup}^3 \tag{15}$$

Where P, Ra and d_p stand for the pressure, average surface roughness, and nanoparticle diameter, respectively. Furthermore, γ is the wall-liquid interaction parameter determined by the surface and liquid materials and β is the surface wettability improvement parameter defined by:

$$\beta = \frac{1 - cos\theta}{1 - cos\theta^*} \tag{16}$$

Where θ and θ* are the liquid contact angles on the nanocoated and clean surfaces, respectively.

Narayan et al. [28] showed that heat transfer by nanofluids was deteriorated when R_a/d_p approaches 1.0; otherwise heat transfer enhanced as $R_a/d_p$was away from 1.0. They proposed when $R_a/d_p$was near 1.0, deposited nanoparticles reduce the active site density. Otherwise, when the surface roughness and particle size were slightly far from more active site density would be created. Therefore, so that the effects of particle size relative to the surface roughness could be effectively considered, Eq. (15) was reformulated by the following expression:

$$N_a = \frac{512}{\gamma} Pr_l^{1.63} \left(14.5 - 4.5 \left(\frac{PR_a}{\sigma} \right) + 0.4 \left(\frac{PR_a}{\sigma} \right)^2 \right) \beta^{-0.4} \xi \left(\frac{R_a}{d_p} \right)^{0.4} \Delta T_{sup}^3 \tag{17}$$

Where

$$\xi \left(\frac{R_a}{d_p} \right) = \begin{cases} 0.275 \left(\frac{R_a}{d_p} \right)^{-1.2} \left(\frac{R_a}{d_p} \right) \leq 1.0 \\ 0.275 + 0.7911 \left(\frac{R_a}{d_p} - 1 \right)^{0.68} \left(\frac{R_a}{d_p} \right) > 1.0 \end{cases} \tag{18}$$

For further survey into achieving a more precise result, Li et al. [19] and Hibiki-Ishii [29] correlations were utilized in this study. The Li correlation (Eq. (19)) is based on experimental data for nanofluid, as follows:

$$N_a = 1.206 \times 10^4 (1 - cos\theta) \Delta T_{sup}^{2.06} \tag{19}$$

Also, Hibiki-Ishii correlation (Eq. (20)) was originally employed for pure water. However, with the following condition it can still be used for nanofluid. These conditions are as follow: 0.101 MPa ≤ P ≤ 19.8 MPa, 5° ≤ θ ≤ 90° and $1 \leq n \leq 1.51 \times 10^6$ sites/cm^2.

$$N_a = \overline{N}_n \left(1 - exp\left(-\frac{\theta^2}{8\zeta^2} \right) \right) \left(exp\left(f(\rho^+) \frac{1}{R_c} \right) - 1 \right) \tag{20}$$

Where

$$R_c = \frac{2\sigma T_{sat}}{\rho_v h_{fg} \Delta T_{sup}} \tag{21}$$

$$f(\rho^+) = -0.01064 + 0.48246\rho^+ - 0.22712\rho^{+2} + 0.05468\rho^{+3} \tag{22}$$

$$\rho^+ = log\frac{\rho_l - \rho_v}{\rho_v} \tag{23}$$

In this correlation, $\overline{N}_n = 4.72 \times 10^5\ sites/m^2$, $\zeta = 0.772$ rad and $l = 2.50 \times 10^{-6}$ m.

The bubble departure diameter is another important nucleate boiling parameter. Formulation of this parameter is challengeable even for pure water. For pure water an empirical correlation by Unal [26] was employed which given by Eq. (24):

$$d_b = 2.42 \times 10^{-5} P^{0.709} \left(\frac{a}{b}\right) \tag{24}$$

where

$$a = \frac{\Delta T_{sup}}{2\rho_v h_{fg}} \sqrt{\frac{\rho_s C_{ps} k_s}{\pi}} \tag{25}$$

$$b = \frac{0.25(\rho_l - \rho_v)}{\rho_l} e^{-0.83} \tag{26}$$

Since there are so many novel features in nanofluid science, achievement of a comprehensive correlation is more complex than pure water. As we attempt to compare the numerical simulation with Gerardi's experimental data, a polynominal correlation that was achieved from fitting Gerardi data by Li et al. [20] was used in this study which is as follows:

$$d_{bw} = -1.91 \times 10^{-3} + 4.21125 \times 10^{-4} \Delta T_{sup} - 1.70945 \times 10^{-5} \Delta T_{sup}^2 + 2.03938 \times 10^{-7} \Delta T_{sup}^3 \tag{27}$$

Finally, for bubble departure frequency, various correlations were suggested in this study. Cole correlation [30], Stephan correlation [31], and Hatton-Hall correlation [32] were investigated in following equations:

$$f = C_f \sqrt{\frac{4g(\rho_l - \rho_v)}{3 d_{bw} \rho_l}} \tag{28}$$

$$f = \frac{1}{\pi} \sqrt{\frac{g}{2 d_{bw}} \left(1 + \frac{4\sigma}{d_{bw}^2 \rho g}\right)} \tag{29}$$

$$f = 284.7 \frac{\lambda_l}{d_{bw}^2 \rho_l C_{p,l}} \tag{30}$$

2.4 The effective properties of nanofluid

Kim et al. [7] found that for dilute nanofluids (concentration of nanoparticles less than 0.1% v), their transport and thermal properties are very similar to those of their base liquids. Also, they revealed that saturation temperature of these nanofluids was within ±1 °C of that of pure water while their surface tension, thermal conductivity and viscosity were negligibly different from those of pure water. Therefore, the following effective properties of nanofluids were used in this study:

Nanofluid density [33]:

$$\rho_{nf} = (1-\varphi)\rho_l + \varphi \rho_{np} \tag{31}$$

Nanofluid viscosity:

$$\mu_{nf} = \left(123\varphi^2 + 7.3\varphi + 1\right)\mu_l \tag{32}$$

Nanofluid specific heat [34]:

$$c_{p,nf} = \frac{(1-\varphi)\rho_l c_{pl} + \varphi \rho_{np} c_{p,np}}{(1-\varphi)\rho_l + \varphi \rho_{nf}} \tag{33}$$

And the Maxwell model for nanofluid thermal conductivity [35]:

$$\frac{k_{nf}}{k_{bf}} = \frac{(1-\varphi)\left(k_{np} + 2k_l\right) + 3\varphi k_{np}}{(1-\varphi)\left(k_{np} + 2k_l\right) + 3\varphi k_l} \tag{34}$$

Where, the subscripts nf, bf and np represent nanofluid, base fluid and nanoparticles respectively and φ is volumetric concentration of nanoparticles in the base fluid.

2.5 Boundary conditions

The aforementioned non-linear and coupled partial differential governing equations were subjected to the following boundary conditions as presentedin Fig. 3.

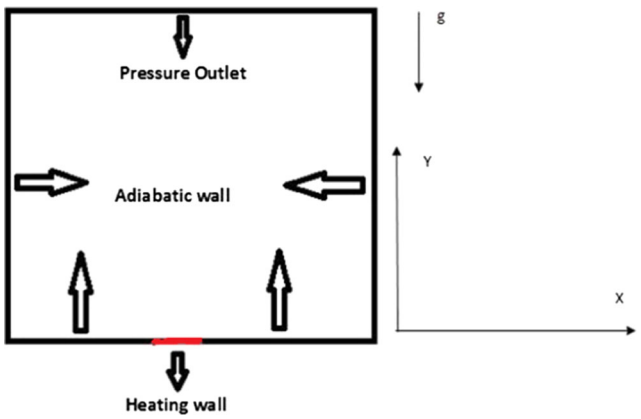

Fig. 3 Schematic of geometry and boundary conditions

At the heating section in the bottom of the enclosure heat flux is constant:

$$\dot{q}''_w = \dot{q}''_{in} \tag{35}$$

At other walls heat flux is zero (adiabatic walls):

$$\dot{q}''_w = -k_w \frac{\partial T}{\partial x} = 0 \tag{36}$$

On top of the vessel the pressure is assumed to be at atmospheric pressure.

$$P = P_{atm} \tag{37}$$

2.6 Numerical method

The two-fluid approach was selected to solve the nucleate pool boiling of silica-water based nanofluid (by 0.1%v). According to Li et al.'s [20], interval of transient initial state was commonly short and nucleate pool boiling of nanofluid was preponderantly characterized by a quasi-steady state. Therefore, modeling of nucleate pool boiling was performed at steady state in this investigation.

The geometry of pool was drawn in 2-D, 400 mm diameter and 200 mm height. This dimension was much larger than the dimension of heating wall (20 mm in diameter), so that the flow and heat transfer is free from the edge effects in the vicinity of the heating section [20]. The domain was then discretized with control volume technique. Several element sizes for meshing were tested. Grid independency test was performed and it was revealed that mesh independence was achieved at 162 × 162 cells. Numerical commutations were performed using CFD code. For the convective and diffusive terms QUICK method (QUICK-type schemes are based on a weighted average of second-order-upwind and central interpolations of the variables) was used, while the SIMPLE procedure was introduced for velocity–pressure coupling. Structured nonuniform grids have been used to discretize the computational domain which were finer in the vicinity of the heated wall where more accurate solutions were necessary. Coverage was attained within 2000 iterations, where the residuals were less than 10^{-6}.

3 Results and discussion

In the first place, the results of numerical simulation for pure water is presented. Eqs. (10), (24), and Eq. (28) were utilized as correlations for active nucleation site density, bubble departure diameter and bubble departure frequency, respectively. Heated wall was presumed smoothly. Thermophysical properties of pure water and nanofluid are presented in Table 1.

Table 1 Thermo-physical properties of pure water and nanofluid

Property	Pure water	Nanofluid
Density of liquid(kg/m^3)	958.000	936.079
Density of vapor (kg/m^3)	0.58	0.58
Dynamic viscosity (pa.s)	0.001	0.001
Thermal conductivity (W/m.k)	0.656	0.661
Specific heat (J/kg.k)	4236	4486
Surface tension (N/m)	0.072	0.072
Liquid contact angle (°)	79	22

Numerical results were compared with experimental data by Gerardi [22] in Fig. 4 which revealed a good agreement with experimental data. This is probably due to the fact that empirical constants of HFP model were based on experimental data of pure water and surface modification does not happen for pure water.

In the next step, numerical simulation was performed for water-silica nanofluid. Volume fraction of silica nanoparticle was selected as 0.1%.In this concentration, nanofluid is hydrodynamically similar to pure water and single phase modeling of liquid phase was reasonable. According to experimental data from Gerardi [22], particle size was 10 nm. Since the deposition of nanoparticles had the most significant effects on bubble nucleation [19] three active site density correlations [Eq. (17), Eq. (19) and Eq. (20)] were used. In the Eq. (13), effect of surface wettability, surface roughness, particle size relative to the surface roughness, and wall superheat were considered. Furthermore, variations of liquid contact angle and wall superheat were considered in Eq. (19) and Eq. (20).

Bubble departure diameter is a challenging subject needing in-depth study for further formulation. Yet there are no comprehensive correlations for this parameter in the literature. For simplicity, the polynomial correlation (Eq. (27)) was used in this study.

Various experiments demonstrated that a larger bubble requires longer time to grow which culminates in a reduced

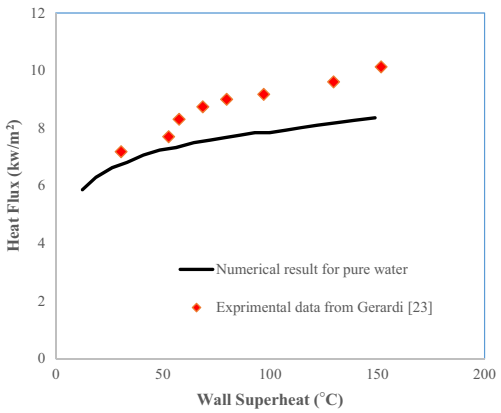

Fig. 4 Comparison of numerical results with experimental data from [22]

Table 2 Equation numbers for HFP model's parameters

Case #	Bubble departure diameter	Frequency of bubble departure	Nucleation site density
1	29	30	19
2	29	30	21
3	29	30	22
4	29	31	19
5	29	31	21
6	29	31	22
7	29	32	19
8	29	32	21
9	29	32	22

bubble departure frequency, and consequently the bubble departure frequency is commonly proportional to reverse bubble departure diameter. Three forms of correlations [Eq. (28), Eq. (29) and Eq. (30)] were employed in numerical simulation. Nevertheless, several runs must be performed to achieve the best model which fits experimental data the most. Table 2 represents the number of runs for various correlations of HFP model.

The results of simulation were depicted in Fig.5. It shows that all numerical simulations were under predicted temperature of wall heating. Case 9 among others had the best agreement with experimental data. These results were achieved for moderate heat fluxes (<200 kW /m^2) at which heat transfer rate increases very rapidly due to the increment of wall superheatand consequently the bubble generating frequency, the enthalpy content of the transient thermal layer and the active nucleation site density increase [36]. Therefore, bubbles are released from the heated wall more quickly and cooler fluid around the bubble flows downward. This fluid flow accelerates the bubbles upward movement. In fact, vorticities circulate fluid under the bubbles and substitute the fresh fluid with the fluid around the heated surface, and operate like a small pump.

At moderate heat fluxes, bubbles grow at isolated nucleation site and do not interact with each other.

Heat transfer coefficient in boiling is calculated using the following relation:

$$h = \frac{q_w}{T_w - T_\infty} \tag{38}$$

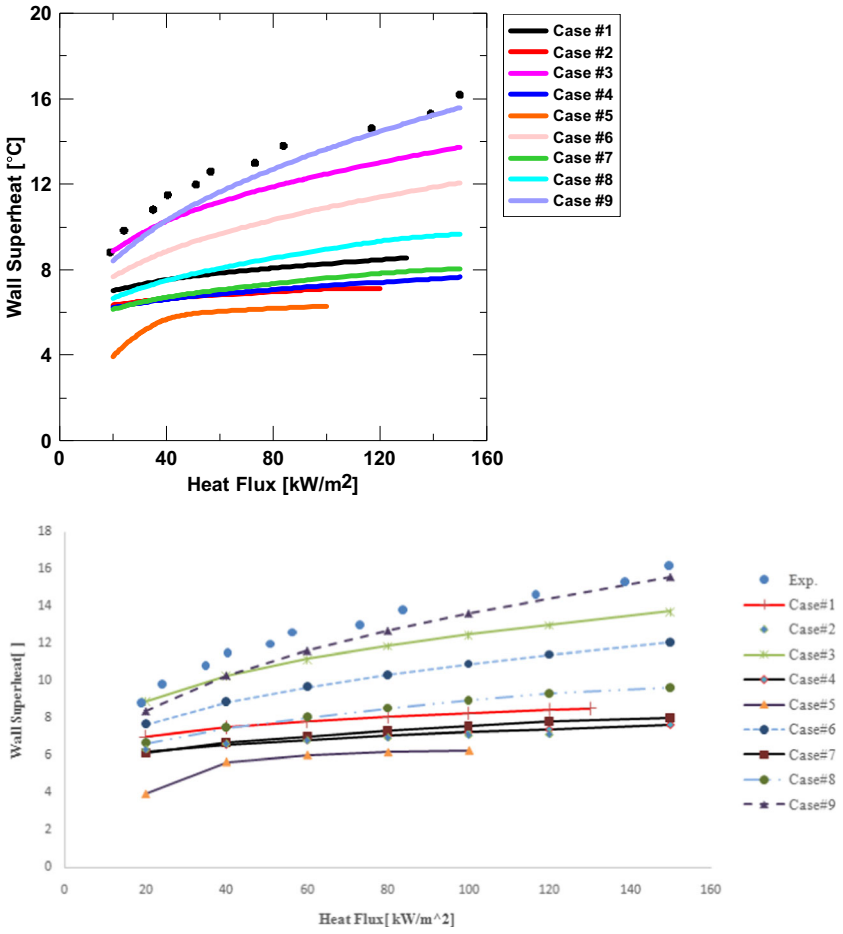

Fig. 5 The results of simulation for different cases

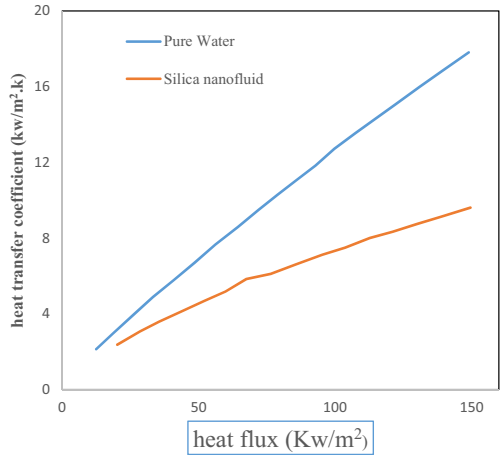

Fig. 6 Comparison of heat transfer coefficient between pure water with silica-water nanofluid

Numerical results of heat transfer coefficient for the model against wall superheat for pure water and nanofluid are depicted in Fig. 6.

As it can be seen, the nucleate boiling heat transfer coefficient for nanofluid was found to decrease. This phenomenon was in agreement with experimental data in the literature. It was related to the surface modification because nanoparticles deposited on the heated wall. In fact, deterioration of heat transfer coefficient was due to notable reduction of bubble departure diameter and nucleation site density. This trend was properly predicted by the HFP model. The reduction of these parameters was a consequence of surface alteration, especially the enhanced surface wettability in the heater surface of boiling nanofluid.

As it is seen in the figure, the model prediction had good agreement with experimental data. These results were achieved using Eq. (16) for nucleation site density. In this correlation, wall superheat and liquid contact angle influenced nucleation site density although Li et al. [20] utilized Eq. (13). It is worthwhile to point out that the ratio of surface roughness to particle diameter of nanoparticle influences nucleation site density. It is perhaps due to roughness variation that appears in the wettability of surface in the presence of nanoparticles. However, Eq. (13) and Eq. (16) are experimentally attained

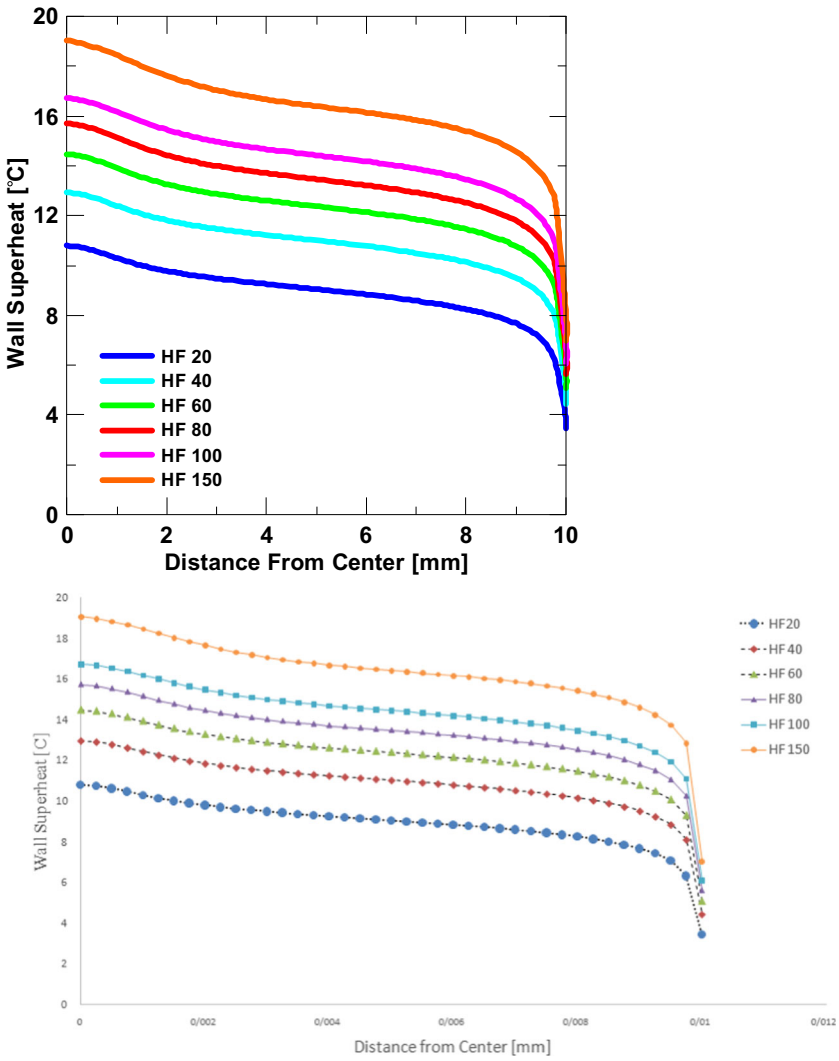

Fig. 7 Temperature distribution along the heater surface in different heat fluxes

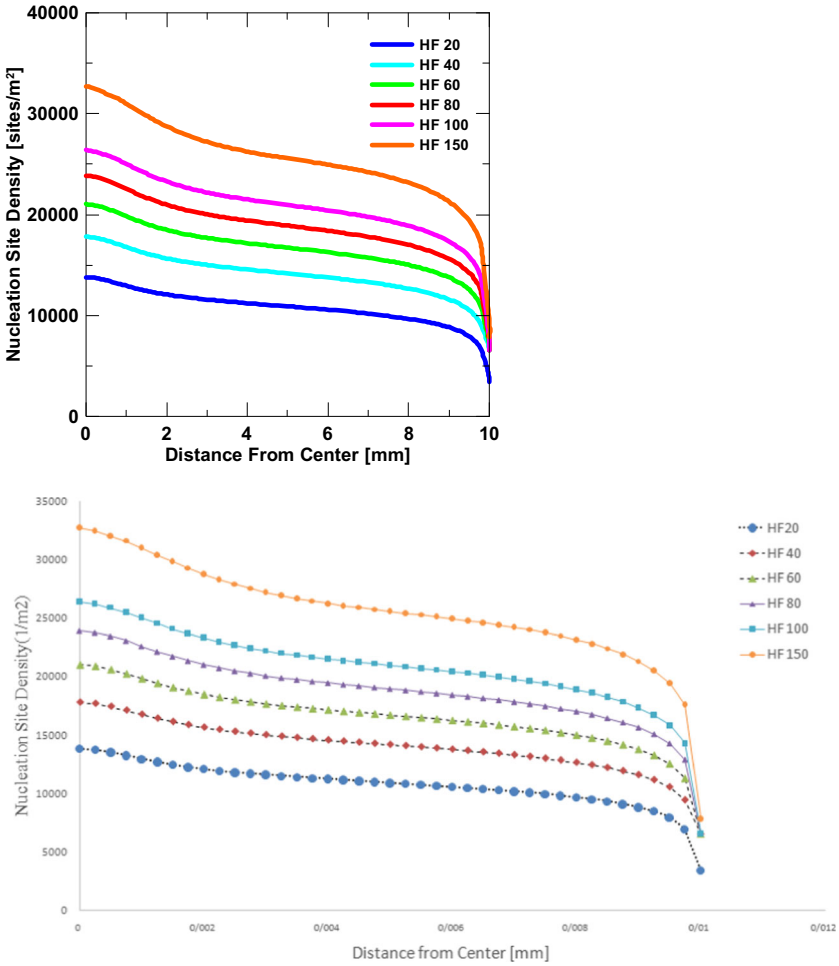

Fig. 8 Nucleation site density distribution along the heater surface in different heat fluxes

and are valid for certain fluids and special condition. Therefore, it is necessary to conduct further investigations in this field. Li correlation from the Gerardi data is the only appropriate correlation for bubble departure diameter in nucleate boiling of nanofluid. More research is needed on bubble departure diameter.

Fig. 7 depicts the temperature distribution along the heater surface in different heat flux. It indicates that temperature increases along the heater. Also, temperature rises with increasing heat flux, and this enhancement has a higher slope at high heat flux values. As it is seen, temperature is maximum in the center and gradually decreases with progress to the edges. When the vapor is in contact with the wall, the temperature of the wall is further from the edges. In the edges of heater, the amount of heat is transferred to the bulk fluid and free convection heat transfer becomes important. Accordingly, this phenomenon is depicted in Fig. 8 in which the distribution of nucleation site density on the surface heater is shown. As it can be seen, the nucleation site density in the center of heater is more than its edges. This means that heat in the center of heater is usually used for evaporation and bubble generation. Away from the center, the bubble generation decreases and amount of heat is transferred to the bulk of fluid by free convection.

Fig. 9 shows variations of bubble departure diameter. From Li correlation, bubble departure diameter depends only on wall superheat. Bubble generation diameter is greater than the edge of heater. With increasing heat flux, the diameter distribution of bubble departure is uniform. Also, frequency of bubble generation is reversely proportional to the bubble diameter. Fig. 10 demonstrates that bubble departure frequency is depicted in distance from center of the heater. As it can be observed, both the bubble detachment frequency as well as bubble detachment diameter were strongly sensitive to the wall superheat. Alternatively, with increase in wall superheat, the bubble grew faster and the time for bubble detachment increased.

4 Conclusion

Numerical simulation of nucleate pool boiling of pure water and dilute water-silica nanofluid (0.1%v) was fulfilled and main remarks were concluded.

Nucleate pool boiling of pure water was modeled by Eulerian two-phase approach. Numerical results were consistent with experimental data.

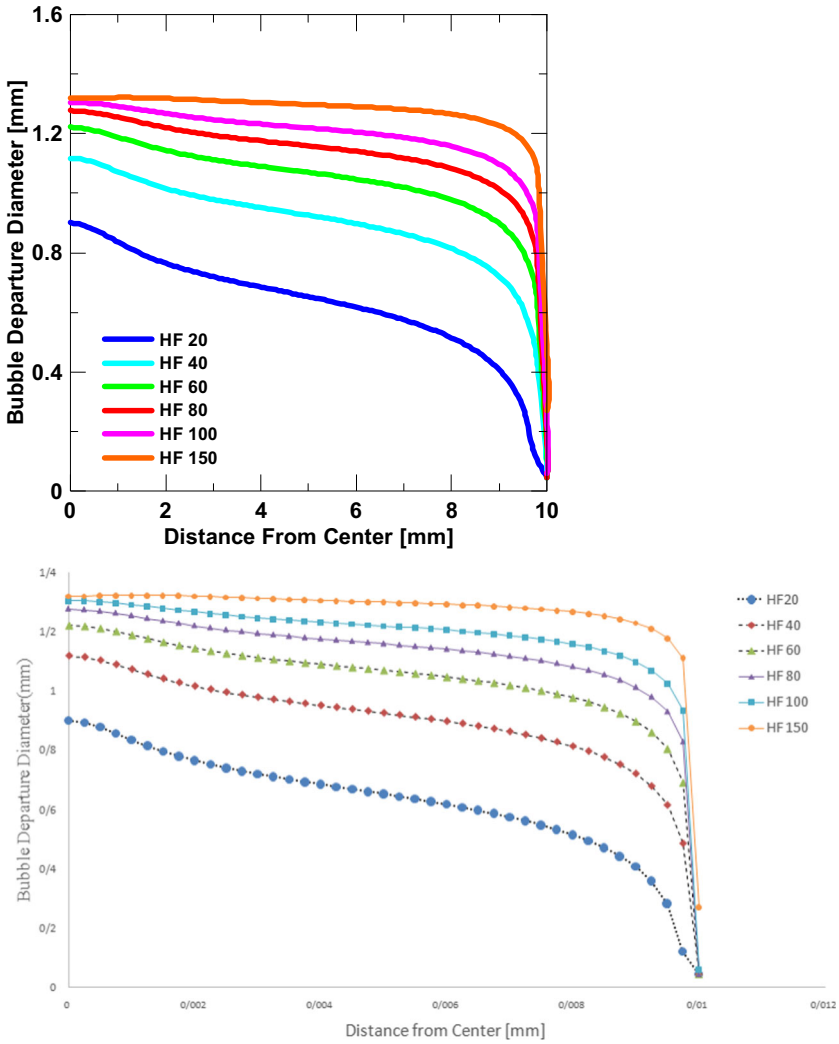

Fig. 9 Bubble departure diameter distribution along the heater surface in different heat fluxes

Nucleate pool boiling of water-silica nanofluid was modeled using multiphase scheme. Due to the very low concentration of nanoparticle in pure water, nanofluid was assumed as a homogenous phase. Therefore, two-phase modeling was reasonable. Various correlations were utilized for active nucleation site density and bubble departure frequency among which Hibiki-Ishii and Hattan-Hall correlations were determined as the best correlations, respectively. Numerical results for this model were in very good agreement with experimental data. Results demonstrated that heat transfer coefficient for nanofluid was

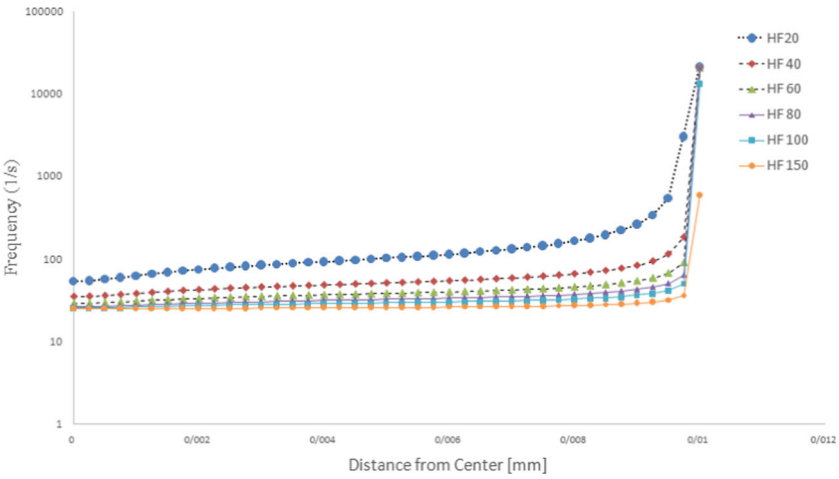

Fig. 10 Bubble detachment frequency distribution along the heater surface in different heat fluxes

lower than pure water. Finally, active nucleation site density, bubble departure diameter, and bubble departure frequency distribution were depicted from the center of the heater. It was revealed these parameters were maximumin the center of the heater. Because much of the heat transferred from the heater to the fluid was consumed for evaporation whereas amount of heat transferred to fluid at the edge was through convection. Owing to the fact that these results were attained for certain nanofluids at specific condition, it is proposed that bubble behavior of nanofluid is experimentally by which a comprehensive model can be achieved. Furthermore, the effect of nanoparticle deposition on liquid contact angle and surface wettability must be investigated in future studies.

References

1. Choi SUS (1995) Enhancement thermal conductivity of fluids with nanoparticles. ASME Fluid Eng Div 231:99–105
2. Bang IC, Kim JH (2010) Thermal-fluid characterizations of ZnO and SiC nanofluids for advanced nuclear power plants. Nucl Technol 170:16–27
3. Khandekar S, Joshi YM, Mehta B (2008) Thermal performance of closed two-phase thermosyphon using nanofluids. Int J Therm Sci 47:659e667
4. Ding GL, Peng H, Jiang WT, Gao YF (2009) The migration characteristics of nanoparticles in the pool boiling process of nano refrigerant and nano refrigerant-oil mixture. Int J Refrig 32:114–123
5. Das SK, Putra N, Roetzel W (2003) Pool boiling characteristics of nano-fluids. Int J Heat Mass Transf 46:851–862
6. You SM, Kim JH, Kim KH (2003) Effect of nanoparticles on critical heat flux ofwater in pool boiling heat transfer. Appl Phys Lett 83:3374–3376
7. Kim SJ, Bang IC, Buongiorno J, Hu LW (2007) Surface wettability change during pool boiling of nanofluids and its effect on critical heatflux. Int J Heat Mass Transf 50:4105–4116
8. Milanova D, Kumar R (2005) Role of ions in pool boiling heat transfer of pure and silica nanofluids. Appl Phys Lett 87:185–194
9. Truong BH (2007) Determination of pool boiling critical heat flux enhancement in nanofluids. Undergraduate THESIS, MIT
10. Sarafraz MM, Hormozi F (2016) Experimental investigation on the pool boiling heat transferto aqueous multi-walled carbon nanotube nanofluids on themicro-finned surfaces. Int J Therm Sci 100:255–266
11. Ciloglu D, Bolukbasi A (2015) A comprehensive review on pool boiling of nanofluids. Appl Therm Eng 84:45–63
12. Kwark SM, Kumar R, Moreno G, Yoo J, You SM (2010) Pool boiling characteristics of low concentration nanofluids. Int J Heat Mass Transf 53:972–981
13. Wen DS, Lin GP, Vafaei S, Zhang K (2009) Review of nanofluids for heat transfer applications. Particuology 7:141–150
14. Congedo PM, Collura S, Congedo PM (2009) Modeling and analysis of natural convection heat transfer in nanofluids. In: HT2008: Proceeding of the Asme Summer Heat Transfer Conference, vol 3, p 569–579
15. Dominguez-Ontiveros E, Fortenberry S, Hassan YA (2010) Experimental observations of flow modifications in nanofluid boiling utilizing particle image velocimetry. Nucl Eng Des 240:299–304
16. Aminfar H, Mohammadpourfard M, Sahraro M (2012) Numerical simulation of nucleate pool boiling on the horizontal surface for nano-fluid using wall heat flux partitioning method. Comput Fluids 66:29–38
17. Ganapathy H, Sajith V (2013) Semi-analytical model for pool boiling of nanofluids. Int J Heat Mass Transf 57:32–47
18. Li XD, Wei W, Wang RS, Shi YM (2009) Numerical and experimental investigation of heat transfer on heating surface during subcooled boiling flow of liquid nitrogen. Int J Heat Mass Transf 52(5–6):1510–1516
19. Li X, Li K, Tu J, Buongiorno J (2014) On two-fluid modeling of nucleate boiling of dilute nanofluids. Int J Heat Mass Transf 69: 443–450
20. Li X, Yuan Y, Jiyuan T (2015) A parametric study of the heat flux partitioning model for nucleate boiling of nanofluids. Int J Therm Sci 98:42–50
21. Valizadeh Z, Shams M (2015) Numerical investigation of water-based nanofluid subcooled flow boiling by three-phase Euler–Euler, Euler–Lagrange approach. Heat Mass Transf 51:601–609
22. Gerardi C, Buongiorno J, Hu L-w, McKrell T (2011) Infrared thermometry study of nanofluid pool boiling phenomena. Nanoscale Res Lett 6:232
23. Nguyen JL (2015) Multiphase Numerical Simulations of Dielectric Fluid Immersion Cooling Scenarios including Effects of Nucleation Site Density and Bubble Departure Diameter Functions. Master's thesis, Auburn University
24. Sato Y, Sadatomi M, Sekoguchi K (1981) Momentum andheat transfer in two-phase bubble flow—I. Int J Multiph Flow 7(2): 167–177
25. Burns AD, Frank T, Hamill I, Shi JM (2004) The Favre averaged drag model for turbulent dispersion in Eulerian multi-phase flows. In: 5th International conference multiphase flow, Yokoshoma, Japan
26. Kocamustafaogullari G, Ishii M (1995) Foundation of the Interfacial Area Transport Equation and its closure relations. Int J Heat Mass Transf 38:481–493
27. Kurul N, Podowski MZ (1990) Multidimensional effects in forced-convection subcooled boiling. In: Heat Transfer 1990, vols 1–7, p 21–26
28. Narayan GP, Anoop KB, Das SK (2007) Mechanism of enhancement/deterioration of boiling heat transfer using stable nanoparticle suspensions over vertical tubes. J Appl Phys 102:074317
29. Hibiki T, Ishii M (2003) Active nucleation site density in boiling systems. Int J Heat Mass Transf 46:2587–2601
30. AEA Technology (1999) CFX-4.3 Solver Manual, Harwell, United Kingdom
31. Stephan K (1992) Heat transfer in condensation and boiling. Springer, New York
32. Hatton AP, Hall IS (1966) Photographic study of boiling on prepared surfaces. In: The 3rd International Heat Transfer Conference, Chicago, Illiois, USA, p 24–37
33. Palm SJ, Roy G, Nguyen CT (2006) Heat transfer enhancement with the use of nanofluids in radial flow cooling systems considering temperature-dependent properties. Appl Therm Eng 26:2209–2218
34. Xuan Y, Roetzel W (2000) Conceptions for heat transfer correlation of nanofluids. Int J Heat Mass Transf 43:3701–3707
35. Yu W, Choi US (2003) The role of international layers in the enhanced thermal conductivity of nanofluids: a renovated Maxwell model. J Nanopart Res 5:167–171
36. Han Y, Griffitht P (1965) The mechanism of heat transfer in nucleate pool boiling boiling-part II. Int J Heat Mass Transf 8:905–914